Adsorption Behavior of Heavy Metal Ions by Hybrid Inulin-TEOS for Water Treatment

Wan Norfazilah Wan Ismail [1*] , Mohamad Irfan Arif Irwan Syah [1], Nur Hanisah Abd Muhet [1], Nurul Hidayah Abu Bakar [1], Hartina Mohd Yusop [1], Nurlin Abu Samah [1]

[1] *Faculty of Industrial Sciences and Technology, Universiti Malaysia Pahang, Lebuhraya Tun Razak, 26300 Gambang, Kuantan, Pahang, Malaysia.*

Abstract

The present work reports the adsorption behavior involved in the adsorption of heavy metal ions using a hybrid inulin-tetraethoxysilane (TEOS) adsorbent produced through the sol-gel process. An aqueous multi-element solution was used in order to examine the inulin-TEOS adsorbent efficiency in removing Cd^{2+}, Co^{2+}, and Ni^{2+} ions. The effects of the contact duration, adsorbent dosage, initial concentration, and solution pH on the adsorption of the targeted metal ions in batch systems were evaluated. The optimal conditions for the removal of all targeted heavy metals were as follows: 30 mg of an adsorbent dosage at pH 4 and 5 minutes of contact time with an initial concentration of 0.5 mg/L. A one-way analysis of variance (one-way ANOVA) with a replication test showed that all parameters had significant differences at a p-value of 0.05. At the optimum condition, 92.59%, 90.27%, and 86.472% of Cd^{2+}, Ni^{2+}, and Co^{2+} were removed, respectively. Findings from kinetic studies suggest that the pseudo-second order model can successfully describe the overall adsorption process. Additionally, the adsorption process can be adequately explained using an intra-particle diffusion model with diffusion rate constants following the sequence of $K_{int,1} > K_{int,2}$ for Co^{2+} and Ni^{2+} and $K_{int,1} > K_{int,2} > K_{int,3}$ for Cd^{2+} in each step. The results suggest that Ni^{2+} fits with the Langmuir isotherm, while Cd^{2+} and Co^{2+} better fit the Freundlich one. Finally, the adsorbent can be reused and is able to retain a good percentage of removal, with percentage difference decreases of 1.99%, 3.29%, and 4.12% for Cd^{2+}, Ni^{2+}, and Co^{2+}, respectively, after the fifth cycle. The hybrid inulin-TEOS bio-sorbent has good adsorption capacity and durability, which could offer a low-cost practical cleaner production process for removing targeted analytes from wastewater.

Keywords: Adsorption; Heavy Metal; Kinetics; Low-Cost Adsorbent; Reusability; Sol-Gel Process.

1. Introduction

Mining, textiles, paper, fertilizer, painting, and petroleum refining industries are considered the main drivers of industrial growth that contribute to the economy and enhance human well-being. Nonetheless, adverse industrial practices have heightened concerns related to water pollution since they are one of the primary contributors to heavy metal ion pollution in water bodies [1–3]. In order to avoid the contamination of public streams and water resources, heavy metals are only allowed to be disposed of in extremely low amounts in wastewater effluent. However, due to their inability to degrade in the environment, heavy metal ions produced by industrial waste will start to accumulate [4, 5] and increased amounts can be absorbed into the cells of living organisms, affecting their physiological and environmental health [6]. To ensure compliance with environmental legal requirements, polluting industries must adequately treat their effluents prior to discharging them to ensure the sustainability of the water supply.

It is vital that an efficient method for the removal of heavy metal ions from wastewater effluents is developed. According to Abuhatab et al. (2020), chemical coagulation, electrocoagulation, bio-sorption, bioremediation, hybrid flotation, and ion exchange have been introduced in recent years to achieve the removal of heavy metals from aqueous solutions. However, because of their high operational costs as well as their ineffectiveness in meeting strict effluent requirements, the adoption rate of these methods has been low [7]. Adsorption has long been acknowledged as one of the most extensively utilized and straightforward methods to remove heavy metals [8]. Additionally, the adsorption of heavy metals or other contaminants using nanoparticles has been recognized as one of the simplest, most reliable, most effective, and lowest-cost methods for water treatment [9–11].

Adsorption occurs when a molecule or ion from a gas or liquid (adsorbate) attaches itself to the surface of a solid or, in rare cases, a liquid (adsorbent). Adsorbents made from natural and renewable materials, particularly biopolymers, have recently piqued researchers' interest due to their ease of availability and their non-toxic nature [12–14]. One of the major advantages of this biopolymer adsorbent is that it can be reused multiple times while still maintaining its efficacy in removing heavy metal ions [15]. Preliminary experiments conducted by Fei et al. (2012), which used cellulose acetate/zeolite (CA/Z) composite fiber, showed that the removal percentage decreased more than 10% for both Cu^{2+} (18.13 %) and Ni^{2+} (12.97 %) after the fifth cycle [16]. While Seunghyun et al. (2021) reported that the performance of polymeric microcapsules (PM) adsorbent on the adsorption of Cu^{2+} ions was around 80% [17]. Another work done by Songlin et al. (2021) was an adsorption-desorption experiment of CO_2-responsive chitosan aerogel adsorbent on Pb^{2+}, Cd^{2+}, CO^{2+}, and Ni^{2+} ions [18]. The results show that desorption rates decrease by more than 20% after the third cycle. Thus, this study was conducted with the aim of producing a low-cost adsorbent with high adsorbent efficiency and better durability for water treatment.

In this study, the efficiency of inulin-silica in the adsorption process under different reaction conditions, namely pH, contact time, initial concentration, and adsorbent dosage, was assessed based on an aqueous sample containing the analyte of interest (Co, Ni, and Cd) to find its optimum value. Additionally, adsorption kinetics were modelled using pseudo-first order, pseudo-second order, and intra-particle diffusion models, while adsorption isotherms were studied using Langmuir and Freundlich isotherms. Finally, the amount of metal ions absorbed and released by the inulin-silica adsorbent after five times of washing was measured to investigate their reusability.

2. Materials and Methods

The adsorbents used in this study were synthesized using solid inulin and liquid tetraethoxysilane (TEOS) as the biopolymer and precursor, respectively; they were purchased from Aladdin, while liquid ethanol (EtOH) and hydrochloric acid (HCl) were obtained from Sigma Aldrich. Nitric acid (HNO_3) and sodium hydroxide (NaOH), purchased from Riendemann Schmidt and R&M Chemicals, respectively, were used to manipulate the pH level. A multi-element solution was used to represent all analytes of interest: Co^{2+}, Ni^{2+}, and Cd^{2+} (Perkin Elmer). Lastly, distilled water was prepared as a solvent in the laboratory.

The synthesis of inulin-silica sol-gel adsorbent was conducted based on previous work [19]. The multi-element calibration standards were diluted in 1% HNO_3. The adsorption of heavy metal ions by inulin-silica was studied via batch experiments at room temperature with all relevant parameters, such as pH, adsorbent dosage, initial concentration, and contact time. The magnetic stirrer was used to agitate the system under study for 60 minutes. After the designated time, the inulin-silica was removed from the aqueous solution using a 0.45 µm nylon syringe filter and transferred into a 12 mL glass vial for the inductively coupled plasma-mass spectrometry (ICP-MS) analysis. The experimental procedure is shown in Figure 1.
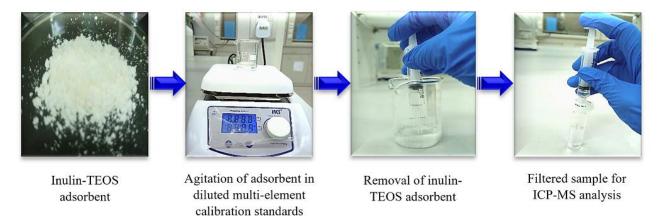

Inulin-TEOS adsorbent → Agitation of adsorbent in diluted multi-element calibration standards → Removal of inulin-TEOS adsorbent → Filtered sample for ICP-MS analysis

Figure 1. The batch experimental for the adsorption of heavy metal ions using inulin-TEOS adsorbent

The percentage removal (%R) of metal ions was calculated using the following formula:

$$\%R = \frac{C_i - C_f}{C_i} \times 100 \tag{1}$$

where C_i (mg/L) is the initial concentration and C_f (mg/L) is the final concentration.

We investigated the influence of the pH on adsorption by altering the pH value from 2 to 5 using 0.1 M nitric acid (HNO_3) and 0.1 M sodium hydroxide (NaOH) using the following criteria: a constant adsorbent dosage of 25 mg, a temperature of 25 °C, a contact period of 60 minutes, and an initial heavy metal concentration of 1.0 mg/L. The optimal dosage of silica-inulin adsorbent was determined by adjusting the dose of inulin-silica from 20.0 to 60.0 mg. The adsorbent was mixed with 1.0 mg/L metal ions in a 10.0 mL aqueous solution at an optimum pH value. The adsorption uptake of the targeted heavy metal ions onto inulin-silica was examined at various predetermined time intervals ranging from 5 to 60 minutes in order to estimate the optimal time required to attain an equilibrium. The optimal inulin-silica dosage and pH were used to investigate the effect of contact time on adsorption with an initial heavy metal concentration of 1.0 mg/L in a 10.0 mL aqueous solution at 25 °C. We examined the applicability of inulin-silica for the removal of metal ions in relation to its initial concentration by adding the optimal inulin-silica dosage to 10 ml of metal ion solution with concentrations of 0.5, 1.0, 1.5, 2.0, and 2.5 mg/L, a temperature of 30 °C and optimal time and pH values. A one-way analysis of variance (one-way ANOVA) using SPSS 26 software was used for data analysis to measure the correlations between the parameters that affect the recovery of the metal ions in aqueous solution.

In this study, three adsorption kinetics were discussed: the pseudo-first-order model, pseudo-second-order model, and intra-particle diffusion. The pseudo-first-order model used the following equation:

$$\log(q_e - q_t) = \log q_e - \frac{k_{p1}}{2.303} t \tag{2}$$

The kinetic data of metal adsorption by the adsorbents were then simulated by the pseudo-second-order model. The equation used for this model is:

$$\frac{t}{q_t} = \frac{1}{k_2 q_e^2} + \frac{t}{q_e} \tag{3}$$

and for intra-particle diffusion, the equation is

$$q_t = k_{int} t^{1/2} + C \tag{4}$$

Two adsorption isotherms, Langmuir and Freundlich, were studied to determine their performance levels. An optimum condition was used with a varying initial metal concentration of 0.5 mg/L, 1.0 mg/L, 1.5 mg/L, 2.0 mg/L, and 2.5 mg/L. The amount of adsorbed metal ions per unit weight of inulin-silica was calculated from the mass balance equation:

$$q_e = \frac{(C_i - C_e)V}{m} \tag{5}$$

where V is the volume of metal ion solution in l, and m is the mass of adsorbent in g.

The Langmuir isotherm can be plotted using the following equation:

$$\frac{C_e}{q_e} = \frac{1}{Q_{max}b} + \frac{C_e}{Q_{max}} \tag{6}$$

As for the Freundlich isotherm, the equation is:

$$\ln q_e = \ln K_f + \left(\frac{1}{n}\right) \ln C_e \tag{7}$$

where, q_e (mg/g) is amount of heavy metal ions adsorbed onto the adsorbent; C_e (mg/L) is the equilibrium concentration of metal ions; Q_{max} (mg/g) is the maximum adsorption capacity; b is the Langmuir constant; K_f (mg/g) is the Freundlich constant, and 1/n is a parameter related to the adsorption intensity.

Sorption-desorption experiments were carried out to assess the reusability of the adsorbent. The experiments were carried out in the following manner: For 15 minutes, 120 mg of inulin-silica adsorbent was in contact with 20 mL of 2 mg/L multielement solution at pH 4.0. The metal-loaded bio-sorbents were later filtered, washed once with deionized water, and dried in oven at 70 °C for 45 min. The procedures were repeated for five cycles of sorption/desorption. The flowchart of experimental procedure is shown in Figure 2.
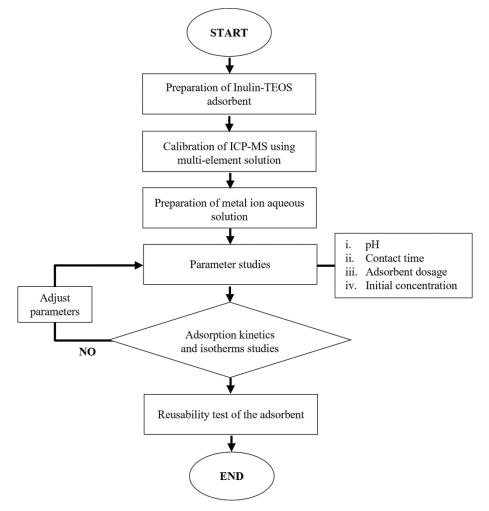
Figure 2. The flowchart of experimental procedure

3. Results and Discussion

3.1. Adsorption Parameters

3.1.1. Effect of pH

Identifying the optimal pH for removing heavy metal via adsorbents is critical to maximize the process, as it affects the: surface charges of adsorbents, the degree of ionization, and the solubility of pollutants [20]. In addition, the pH may alter the electrostatic interactions between the absorbent and pollutants due to having the opposite surface charge [21]. Figure 3 shows the influence of the pH on the inulin-silica removal efficiency when removing the targeted analytes from a multi-element standard solution with pH values ranging from 2 to 5. When the pH was raised from 2 to 4, the metal uptake rose and when the pH was increased above 4, it declined. At pH 2, the removal efficiency was 85.49%, 81.88%, and 80.39% and these values increased to 94.03%, 91.48%, and 89.06% for Cd, Ni, and Co, respectively, at pH 4.

According to Wadhawan et al. (2020), this is associated with the existence of large concentrations of H^+ and H_3O^+ ions at low pH values which compete for active binding sites with heavy metal ions for adsorption [22] and its leading to the declination in electrostatic interaction to some extent [23]. Therefore, increasing the pH level leads to greater efficiency in metal removal due to the greater presence of OH groups at the adsorbent surface sites, causing less competition between proton ions (H^+) and metal ions as the electrostatic interaction dominated the adsorption behavior [24, 25]. However, in the experiment, when the pH value exceeded 4, there was a clear reduction in the removal efficiency of the adsorbent, likely due to hydroxide ions in the solution precipitating the metal ions and forming $Co(OH)_2$, $Cd(OH)_2$ and $Ni(OH)_2$ [6]. This result is associated with the adsorption behavior of modified cellulose-chitosan adsorbent [26], cellulose acetate/zeolite composite fiber adsorbent [16], and silica nanotubes (SNTs) adsorbent [23], as the trends for absorption percentage of heavy metal ions decrease with increasing of pH more than 4. Thus, pH 4 was chosen as the optimal level to eliminate any potential precipitate.
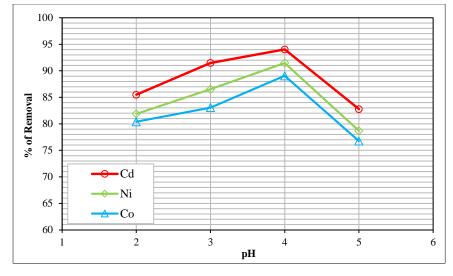
Figure 3. Effect of pH on percentage (%) removal of metal ions

3.1.2. Effect of the Adsorbent Dosage

The interaction between metal ions and adsorbent sites in the solution can be maximized by obtaining an optimal adsorbent dosage. The impact of the adsorbent dose on the adsorption effectiveness of Co, Cd, and Ni onto inulin-silica is illustrated in Figure 4. It was observed that the removal efficiency improved when the doses of inulin-silica increased from 20 to 30 mg, whereas further increases in the adsorbent dosage resulted in slightly decreasing and constant trends. This could be due to the fact that increasing the dosage can increase the number of active adsorption sites, resulting in a higher removal efficiency [6]. Meanwhile, because unsaturated sites are present during the process, this will inadvertently lower the total amount of heavy metals absorbed per unit mass of an adsorbent [27]. In addition, increasing inulin-silica dosages with no changes in the agitation speed may promote some aggregation in the system that is overlapping the nanoparticles. Thus, there are fewer binding sites accessible for metal ions to bind to at higher inulin-silica doses [24]. The experimental results show that the adsorbate percentage removal was the highest at 30 mg with values of 93.52%, 93.62%, and 92.02% for Cd, Ni, and Co, respectively. Hence, 30 mg of inulin-silica was chosen as the best adsorbent for further testing.
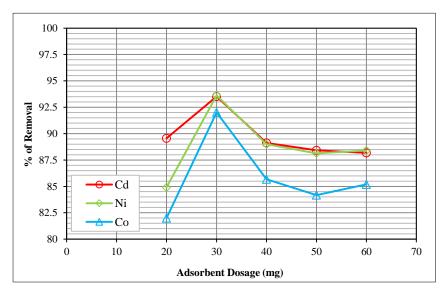

Figure 4. Effect of the adsorbent dosage on % removal of metal ions

3.1.3. Effect of Contact Time

Equilibrium time is an important factor in developing a cost-effective wastewater treatment process as it (contact time) may affect both the economic efficiency and adsorption kinetics of the process. If the adsorbents have to bind to all of the available active sites on the surface of the adsorbent, a further increase in contact time will no longer increase the removal of heavy metal ions and may even contribute to its decrease [28]. In other words, the percentage of adsorption increased with time until saturation, as it is subjected to the amount of heavy metal ions transported to inulin-TEOS active sites [29]. The effect of contact time on the adsorption of ions onto inulin-silica is shown in Figure 5. An

extended contact period does not lead to greater efficiency and, instead, the desorption of adsorbed ions may be promoted with longer contact times and a lower adsorption efficiency may occur [30]. Thus, the optimal contact time for further study is 5 minutes. Over this duration, the metal ion removal efficiency is maximized: 91.43% for Cd, 89.97% for Ni, and 88.44% for Co. The difference in the ion-exchange capacity of the heavy metal ions on adsorbent resulting in the different of removal efficiency of inulin-TEOS adsorbent [31].
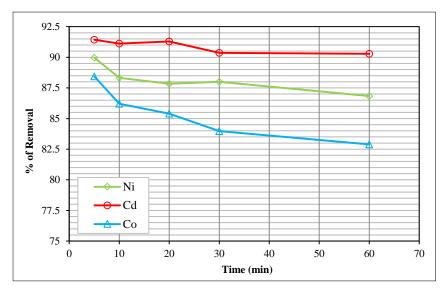

Figure 5. Effect of contact time on % removal of metal ions

3.1.4. Effect of the Initial Concentration

Metal ion solutions with varying initial concentrations were equilibrated using a 30 mg adsorbent dose. Figure 6 shows that the metal ion removal efficiency decreased from 92.59, 90.27, and 86.47 to 88.99, 79.73, and 76.37% for Cd, Ni, and Co, respectively when the initial concentration was increased from 0.5 mg/L to 2.5 mg/L. The reason for this is that there were large surface and adsorption sites available at lower initial solution concentrations, prompting the ions to be rapidly adsorbed and removed. However, higher initial solution concentrations constrained the availability of adsorption sites, which led to a decline in the percentage removal, most likely as a result of the saturation of adsorption sites on the surface of the adsorbent which could not accommodate the higher concentration of metal ion solutions [32]. Even though metal ion removal efficiency was reduced as the initial concentration was increased, the change was minor at concentrations ranging from 0.5 to 2.5 mg/L. The percentage of removal reduced from 92.59 to 88.99% for Cd, 90.28 to 79.73% for Ni, and 86.47 to 76.37% for Co. This indicates that the initial concentration only had a small impact on the adsorption [33]. The current study, therefore, found that the optimal initial concentration for the removal of Cd, Co, and Ni was 0.5 mg/L. Results obtained from this study is distinctly differ from previous study by Ouyang et al (2019) which used silicate porous material adsorbent in terms of adsorption capacity as it was sharply increased with the increasing of the initial concentration of metal ions [31].
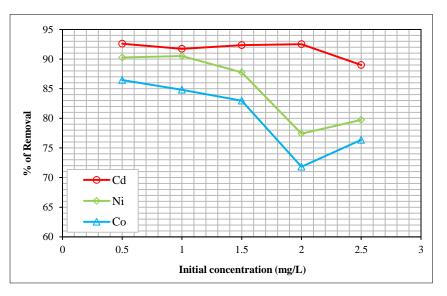

Figure 6. Effect of the initial concentration on % removal of metal ions

To assess the significance of the results obtained in this study, an ANOVA was conducted for all parameters (effect of adsorbent dosage, initial concentration of metal ions, pH, and contact time on the adsorption of metal ions onto inulin-silica). The single-factor ANOVA test was used because all parameters were optimized using the classical one variable at a time (OVAT) methodology. The results of the single factor ANOVA show that all parameters measured in this study had significant differences ($P < 0.05$) regarding the removal of selected heavy metal ions onto the inulin-silica adsorbent.

3.2. Adsorption Kinetics

3.2.1. Pseudo First and Second Order

The kinetics of adsorption shows the rate of metal ions uptake onto the inulin-silica material by implementing the pseudo-first order or pseudo-second order models under the identical set of experimental parameters for optimal contact time studies. Table 1 lists the kinetic parameters derived from both models.

Table 1. Kinetic adsorption parameters obtained using pseudo-first order and pseudo-second order models

Metal ion	Pseudo-first order			Pseudo-second order		
	k	q_e	R^2	k	q_e	R^2
Cd	0.0960	258404.46	0.697	3×10^{-7}	2×10^6	0.9957
Co	0.0606	4979663.54	0.957	4×10^{-8}	11×10^6	0.9982
Ni	0.0359	420532.92	0.6205	1×10^{-6}	1×10^6	0.9971

The model's fitness was assessed based on the correlation coefficient values obtained for each kinetic model. Table 1 shows that the pseudo-second order kinetic model was better at modelling the kinetic data than the pseudo-first order kinetic model, with all R^2 values being beyond 0.995. In general, the pseudo-first order model does not function well over a wide range of contact times, and it is only useful in the early stages of adsorption. It is, therefore, not suitable for the entire adsorption period [34]. The assumption behind the pseudo-second order rate is that chemical adsorption is the rate-limiting process [28]. According to Ali et al. (2016), as adsorption follows the pseudo-second order model, the governing mechanism in the adsorption of these three contaminants is chemisorption, which produces valency forces by sharing or exchanging electrons between the adsorbent and adsorbate [35]. The chemical reaction between inulin-TEOS adsorbent and heavy metal ions mainly arose from the complexation of metal ions via the hydroxyl group in the molecular structure of inulin-TEOS [19].

3.2.2. Intra-Particle Diffusion Model

The inulin-silica pores used in this study ranged in size from 2 to 50 nm [19]. Due to the mesoporous structure of the inulin-silica adsorbents, diffusion was predicted to control the adsorption rate [36]. Thus, even though the pseudo-second-order equation fits best with the current experimental data, the model is inefficient at forecasting the diffusion process. The effect of diffusion was studied using the Weber–Morris model. Figure 7 shows the fitting of the inter-particle diffusion model for the adsorption of the various metal ions, whereby the intra-particle model plot has more than one linear region depicting the mass transfer of inulin-silica. The distinct stages of diffusion can be attributed to these regions. The slope of the plots might be used to calculate the intra-particle diffusion constants. $K_{int,1}$, $K_{int,2,}$ and $K_{int,3}$, which represent the diffusion rates of the different stages in the adsorption process, are described in Table 2.
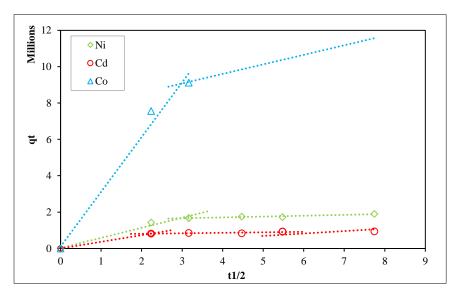

Figure 7. Intra-Particle Diffusion Model

Table 2. Intra-particle diffusion model parameters for metal adsorption

Metal ion	Intra-particle diffusion model		
	$K_{int,1}$	$K_{int,2}$	$K_{int,3}$
Cd	365338	27571	3558
Ni	549198	47799	0
Co	3×10^6	523647	0

Co^{2+} and Ni^{2+} represent a linear line that is divided into two linear plots to reveal a two-stage process. The first plot implies that the metal ions are mass transferred from the solution to the boundary layer of the solid adsorbent, while the second plot represents metal ion adsorption into the pore surface of adsorbents [37]. However, for the adsorption of Cd^{2+}, the process is divided into three stages. As stated by Zhang et al. (2019), a boundary layer effect is demonstrated by the surface diffusion and adsorption in the initial phase [38]. Ren at al. (2013) stated that, when the adsorption of the exterior active site is almost occupied or saturated, metal ions enter the adsorbent's pores and are absorbed by the mesopores' inner surfaces, as seen in the second stage [39]. The diffusion resistance rises when heavy metal ions enter the pores, resulting in a drop in the diffusion rate [40]. According to Repo et al. (2011), in the third linear plot, when the solute concentration quickly declines, the intra-particle diffusion rate constants are close to zero, indicating that diffusion into micropores is taking place or has reached an equilibrium stage [41].

When the linear regressions do not pass through the origin, it can be inferred that -particle diffusion is not the sole rate-determining step in controlling the adsorption process [38]; rather, it indicates the boundary layer thickness [37]. Hence, it is expected that both film diffusion and intra-particle diffusion are involved in the adsorption process [36]. The diffusion rate constants follow the sequence of $K_{int,1} > K_{int,2}$ for Co^{2+} and Ni^{2+} and $K_{int,1} > K_{int,2} > K_{int,3}$ for Cd^{2+} in each step.

3.3. Adsorption Isotherms

3.3.1. Langmuir and Freundlich isotherms

The R^2 values of the Langmuir and Freundlich isotherm model were used to assess the adsorption mechanism of the composite membrane. The Langmuir isotherm suggests that monolayer adsorption of metal ions happens on the same active sites on the surface of the adsorbent. This is due to the fact that the sites are uniform and have the same energy levels [42]. The Freundlich isotherm suggests that the adsorbent's surface is heterogeneous, which supports the fact that adsorption occurs on a surface made up of heterogeneous patches [43]. The results of the experiment are shown in Table 3.

Table 3. Langmuir and Freundlich isotherm parameters

Metal ion	Langmuir Model			Freundlich Model		
	q_{max} (mg/g)	b (L/mg)	R^2	1/n	K_f (mg/g)	R^2
Cd	1.8961	2.5739	0.7414	1.0740	2.54×10^{-4}	0.9243
Co	0.9463	2.1951	0.8525	2.3832	1.45×10^{-3}	0.9795
Ni	0.8288	5.2781	0.9293	1.3959	8.82×10^{-4}	0.8438

It is clear from the results shown in Table 3 that the adsorption behaviour fits the Freundlich isotherm. The adsorption process takes place on the membrane surface as a result of the interaction of metal ions with a number of the composite membrane's functional groups. The process is assumed to occur on a membrane surface that is heterogeneous and has a different level of adsorption energy (due to surface roughness) [44, 45]. This is associated with our previous study that showed the inulin-TEOS adsorbent has a rough surface with the presence of irregular pores due to the presence of TEOS [19]. Ni^{2+} was shown to better fit with the Langmuir isotherm model, suggesting that they undergo monolayer adsorption. The Langmuir model assumes that there is a given number of adsorption sites on the surface in the beginning and that adsorption is limited to monolayer coverage and that the energy change is constant [46]. Thus, no adsorption will take place under equilibrium conditions.

3.4. Reusability of the Adsorbent

Stability under a variety of conditions influences an adsorbent's economic and environmental performance. In this study, the adsorption–desorption cycle was performed five times to test the reusability of inulin-silica (the results are shown in Figure 8). After the fifth cycle, the removal percentage decreased by 1.99 %, 3.29 %, and 4.12 % for Cd, Ni, and Co, respectively, which could be attributed to adsorbent loss during the washing processes after each adsorption–desorption cycle was completed [27]. According to Cho et al. (2021), the strong interaction between the heavy metal ions and the surface of absorbance leads to the decrease of active sites, which could explain the reduction of the

desorption process. They also added that the co-existing cations in the adsorption process could be another factor for the reduction of the removal percentage of heavy metal ions [17]. However, the small decrease after the fifth cycle suggests that inulin-silica may be regenerated and that it retains a high removal percentage, so it could be used in the industry as an effective adsorbent.
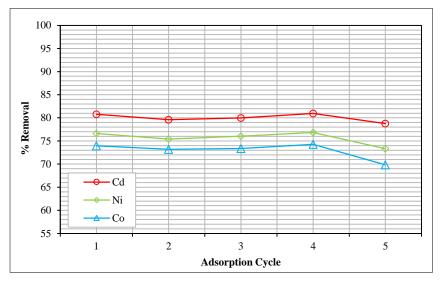

Figure 8. Reusability of adsorbent

4. Conclusion

In this study, the adsorption behavior and interaction mechanism of Co^{2+}, Cd^{2+}, and Ni^{2+} onto the hybrid inulin-TEOS adsorbent were studied. The process was achieved with a shorter contact time and high removal capacity, indicating its efficacy, which could be a better alternative to conventional adsorbents. The investigation found that the adsorption performance was greatly affected by the pH value and the presence of heavy metal ions in the solution. The removal rates of metal ions increase with the increase of pH from 2 to 4, and they decrease above pH 4. The selective adsorption of the metals occurred in the following order: $Cd^{2+} > Ni^{2+} > Co^{2+}$. The Freundlich model was found to provide better results for the adsorption process. The optimum adsorption capacity for Co^{2+} and Cd^{2+} occurred on a rough surface and without functional groups, while a uniform surface topography fitted better for the Langmuir model of Ni^{2+} on the adsorbent surface. The kinetic model fitting results indicate that heavy metal ion diffusion and chemical adsorption are the rate-limiting processes. The removal mechanisms were mainly attributed to the ion exchange process and hydroxyl groups on the hybrid inulin-TEOS surface. Based on the good absorption capacity, durability, and economics, inulin-TEOS adsorbent could be a future prospect in the wastewater treatment industry. However, further research on its adsorption capability in the actual wastewater environment should be considered in order to increase its environmental relevance. Technically, this work provides a better understanding of the adsorption mechanism of heavy metals to control water pollution.

5. Declarations

5.1. Author Contributions

Conceptualization, W.N.W.I.; methodology, M.I.A.I.S., and N.H.A.M.; validation, W.N.W.I., N.A.S., and H.M.Y.; formal analysis, W.N.W.I., M.I.A.I.S, N.H.A.M., and H.M.Y.; investigation, M.I.A.I.S., and N.H.A.M.; resources, W.N.W.I.; data curation, N.H.A.B., M.I.A.I.S., and N.H.A.M.; writing—original draft preparation, W.N.W.I., M.I.A.I.S., and N.H.A.M.; writing—review and editing, W.N.W.I., N.A.S., H.M.Y., and N.H.A.B.; supervision, W.N.W.I.; project administration, W.N.W.I.; funding acquisition, W.N.W.I. All authors have read and agreed to the published version of the manuscript.

5.2. Data Availability Statement

The data presented in this study are available in the article.

5.3. Funding

5.4. Acknowledgements

5.5. Conflicts of Interest

The authors declare no conflict of interest.

6. References

[1] Rezapour, S., Siavash Moghaddam, S., Nouri, A., & Khosravi Aqdam, K. (2022). Urbanization influences the distribution, enrichment, and ecological health risk of heavy metals in croplands. Scientific Reports, 12(1), 3868. doi:10.1038/s41598-022-07789-x.

[2] Shi, X. M., Liu, S., Song, L., Wu, C. S., Yang, B., Lu, H. Z., Wang, X., & Zakari, S. (2022). Contamination and source-specific risk analysis of soil heavy metals in a typical coal industrial city, central China. Science of the Total Environment, 836, 155694. doi:10.1016/j.scitotenv.2022.155694.

[3] Zhao, H., Wu, Y., Lan, X., Yang, Y., Wu, X., & Du, L. (2022). Comprehensive assessment of harmful heavy metals in contaminated soil in order to score pollution level. Scientific Reports, 12(1), 3552. doi:10.1038/s41598-022-07602-9.

[4] Mansoor, S., Kour, N., Manhas, S., Zahid, S., Wani, O. A., Sharma, V., Wijaya, L., Alyemeni, M. N., Alsahli, A. A., El-Serehy, H. A., Paray, B. A., & Ahmad, P. (2021). Biochar as a tool for effective management of drought and heavy metal toxicity. Chemosphere, 271, 129458. doi:10.1016/j.chemosphere.2020.129458.

[5] Khoso, W. A., Haleem, N., Baig, M. A., & Jamal, Y. (2021). Synthesis, characterization and heavy metal removal efficiency of nickel ferrite nanoparticles (NFN's). Scientific Reports, 11(1), 3790. doi:10.1038/s41598-021-83363-1.

[6] Betiha, M. A., Moustafa, Y. M., El-Shahat, M. F., & Rafik, E. (2020). Polyvinylpyrrolidone-Aminopropyl-SBA-15 Schiff Base hybrid for efficient removal of divalent heavy metal cations from wastewater. Journal of Hazardous Materials, 397, 122675. doi:10.1016/j.jhazmat.2020.122675.

[7] Abuhatab, S., El-Qanni, A., Al-Qalaq, H., Hmoudah, M., & Al-Zerei, W. (2020). Effective adsorptive removal of Zn^{2+}, Cu^{2+}, and Cr^{3+} heavy metals from aqueous solutions using silica-based embedded with NiO and MgO nanoparticles. Journal of Environmental Management, 268, 110713. doi:10.1016/j.jenvman.2020.110713.

[8] Kumar, R., Barakat, M. A., Daza, Y. A., Woodcock, H. L., & Kuhn, J. N. (2013). EDTA functionalized silica for removal of Cu(II), Zn(II) and Ni(II) from aqueous solution. Journal of Colloid and Interface Science, 408(1), 200–205. doi:10.1016/j.jcis.2013.07.019.

[9] Manzoor, K., Ahmad, M., Ahmad, S., & Ikram, S. (2019). Removal of Pb(ii) and Cd(ii) from wastewater using arginine cross-linked chitosan-carboxymethyl cellulose beads as green adsorbent. RSC Advances, 9(14), 7890–7902. doi:10.1039/C9RA00356H.

[10] Vinayagam, V., Murugan, S., Kumaresan, R., Narayanan, M., Sillanpää, M., Vo, D. V. N., & Kushwaha, O. S. (2022). Protein nanofibrils as versatile and sustainable adsorbents for an effective removal of heavy metals from wastewater: A review. Chemosphere, 301, 134635. doi:10.1016/j.chemosphere.2022.134635.

[11] Uko, C. A., Tijani, J. O., Abdulkareem, S. A., Mustapha, S., Egbosiuba, T. C., & Muzenda, E. (2022). Adsorptive properties of MgO/WO_3 nanoadsorbent for selected heavy metals removal from indigenous dyeing wastewater. Process Safety and Environmental Protection, 162, 775–794. doi:10.1016/j.psep.2022.04.057.

[12] Akinterinwa, A., Reuben, U., Atiku, J. U., & Adamu, M. (2022). Focus on the removal of lead and cadmium ions from aqueous solutions using starch derivatives: A review. Carbohydrate Polymers, 290, 119463. doi:10.1016/j.carbpol.2022.119463.

[13] Li, W., Qamar, S. A., Qamar, M., Basharat, A., Bilal, M., & Iqbal, H. M. N. (2021). Carrageenan-based nano-hybrid materials for the mitigation of hazardous environmental pollutants. International Journal of Biological Macromolecules, 190, 700–712. doi:10.1016/j.ijbiomac.2021.09.039.

[14] adav, M., Gupta, R., & Sharma, R. K. (2019). Green and Sustainable Pathways for Wastewater Purification. Advances in Water Purification Techniques, 355–383, Elsevier, Amsterdam, Netherlands. doi:10.1016/b978-0-12-814790-0.00014-4.

[15] Younas, F., Mustafa, A., Farooqi, Z. U. R., Wang, X., Younas, S., Mohy-Ud-din, W., Hameed, M. A., Abrar, M. M., Maitlo, A. A., Noreen, S., & Hussain, M. M. (2021). Current and emerging adsorbent technologies for wastewater treatment: Trends, limitations, and environmental implications. Water (Switzerland), 13(2), 215. doi:10.3390/w13020215.

[16] Ji, F., Li, C., Tang, B., Xu, J., Lu, G., & Liu, P. (2012). Preparation of cellulose acetate/zeolite composite fiber and its adsorption behavior for heavy metal ions in aqueous solution. Chemical Engineering Journal, 209, 325–333. doi:10.1016/j.cej.2012.08.014.

[17] Cho, S., Kim, J. H., Yang, K. S., & Chang, M. (2021). Facile preparation of amino-functionalized polymeric microcapsules as efficient adsorbent for heavy metal ions removal. Chemical Engineering Journal, 425, 130645. doi:10.1016/j.cej.2021.130645.

[18] Fan, S., Chen, J., Fan, C., Chen, G., Liu, S., Zhou, H., Liu, R., Zhang, Y., Hu, H., Huang, Z., Qin, Y., & Liang, J. (2021). Fabrication of a CO_2-responsive chitosan aerogel as an effective adsorbent for the adsorption and desorption of heavy metal ions. Journal of Hazardous Materials, 416, 126225. doi:10.1016/j.jhazmat.2021.126225.

[19] Yusop, H. M., Ismail, A. I. H. M., & Ismail, W. N. W. (2021). Preparation and characterization of new sol–gel hybrid inulin–teos adsorbent. Polymers, 13(8), 1295. doi:10.3390/polym13081295.

[20] Akpomie, K. G., & Conradie, J. (2020). Efficient synthesis of magnetic nanoparticle-Musa acuminata peel composite for the adsorption of anionic dye. Arabian Journal of Chemistry, 13(9), 7115–7131. doi:10.1016/j.arabjc.2020.07.017.

[21] Tee, G. T., Gok, X. Y., & Yong, W. F. (2022). Adsorption of pollutants in wastewater via biosorbents, nanoparticles and magnetic biosorbents: A review. Environmental Research, 212, 113248. doi:10.1016/j.envres.2022.113248.

[22] Wadhawan, S., Jain, A., Nayyar, J., & Mehta, S. K. (2020). Role of nanomaterials as adsorbents in heavy metal ion removal from waste water: A review. Journal of Water Process Engineering, 33, 101038. doi:10.1016/j.jwpe.2019.101038.

[23] Wang, P., Du, M., Zhu, H., Bao, S., Yang, T., & Zou, M. (2015). Structure regulation of silica nanotubes and their adsorption behaviors for heavy metal ions: PH effect, kinetics, isotherms and mechanism. Journal of Hazardous Materials, 286, 533–544. doi:10.1016/j.jhazmat.2014.12.034.

[24] Sherlala, A. I. A., Raman, A. A. A., Bello, M. M., & Buthiyappan, A. (2019). Adsorption of arsenic using chitosan magnetic graphene oxide nanocomposite. Journal of Environmental Management, 246, 547–556. doi:10.1016/j.jenvman.2019.05.117.

[25] Tang, S., Lin, L., Wang, X., Yu, A., & Sun, X. (2021). Interfacial interactions between collected nylon microplastics and three divalent metal ions (Cu(II), Ni(II), Zn(II)) in aqueous solutions. Journal of Hazardous Materials, 403, 123548. doi:10.1016/j.jhazmat.2020.123548.

[26] Rahaman, M. H., Islam, M. A., Islam, M. M., Rahman, M. A., & Alam, S. M. N. (2021). Biodegradable composite adsorbent of modified cellulose and chitosan to remove heavy metal ions from aqueous solution. Current Research in Green and Sustainable Chemistry, 4, 100119. doi:10.1016/j.crgsc.2021.100119.

[27] Zaimee, M. Z. A., Sarjadi, M. S., & Rahman, M. L. (2021). Heavy metals removal from water by efficient adsorbents. Water (Switzerland), 13(19), 2659. doi:10.3390/w13192659.

[28] Hassan, A. M., Wan Ibrahim, W. A., Bakar, M. B., Sanagi, M. M., Sutirman, Z. A., Nodeh, H. R., & Mokhter, M. A. (2020). New effective 3-aminopropyltrimethoxysilane functionalized magnetic sporopollenin-based silica coated graphene oxide adsorbent for removal of Pb(II) from aqueous environment. Journal of Environmental Management, 253, 109658. doi:10.1016/j.jenvman.2019.109658.

[29] Duan, P., Yan, C., Zhou, W., & Ren, D. (2016). Development of fly ash and iron ore tailing based porous geopolymer for removal of Cu(II) from wastewater. Ceramics International, 42(12), 13507–13518. doi:10.1016/j.ceramint.2016.05.143.

[30] Tembhurkar, A. R., & Deshpande, R. (2012). Powdered Activated Lemon Peels as Adsorbent for Removal of Cutting Oil from Wastewater. Journal of Hazardous, Toxic, and Radioactive Waste, 16(4), 311–315. doi:10.1061/(asce)hz.2153-5515.0000132.

[31] Ouyang, D., Zhuo, Y., Hu, L., Zeng, Q., Hu, Y., & He, Z. (2019). Research on the adsorption behavior of heavy metal ions by porous material prepared with silicate tailings. Minerals, 9(5), 291. doi:10.3390/min9050291.

[32] Prajapati, A. K., Verma, P., Singh, S., Mondal, M. K., & Kooh, M. R. R. (2022). Adsorption-Desorption Surface Bindings, Kinetics, and Mass Transfer Behavior of Thermally and Chemically Treated Great Millet Husk towards Cr(VI) Removal from Synthetic Wastewater. Adsorption Science and Technology, 2022, 1–16. doi:10.1155/2022/3956977.

[33] Padmavathy, K. S., Madhu, G., & Haseena, P. V. (2016). A study on Effects of pH, Adsorbent Dosage, Time, Initial Concentration and Adsorption Isotherm Study for the Removal of Hexavalent Chromium (Cr (VI)) from Wastewater by Magnetite Nanoparticles. Procedia Technology, 24, 585–594. doi:10.1016/j.protcy.2016.05.127.

[34] Repo, E., Kurniawan, T. A., Warchol, J. K., & Sillanpää, M. E. T. (2009). Removal of Co(II) and Ni(II) ions from contaminated water using silica gel functionalized with EDTA and/or DTPA as chelating agents. Journal of Hazardous Materials, 171(1–3), 1071–1080. doi:10.1016/j.jhazmat.2009.06.111.

[35] Ali, R. M., Hamad, H. A., Hussein, M. M., & Malash, G. F. (2016). Potential of using green adsorbent of heavy metal removal from aqueous solutions: Adsorption kinetics, isotherm, thermodynamic, mechanism and economic analysis. Ecological Engineering, 91, 317–332. doi:10.1016/j.ecoleng.2016.03.015.

[36] Repo, E., Warchoł, J. K., Bhatnagar, A., & Sillanpää, M. (2011). Heavy metals adsorption by novel EDTA-modified chitosan-silica hybrid materials. Journal of Colloid and Interface Science, 358(1), 261–267. doi:10.1016/j.jcis.2011.02.059.

[37] Gupta, R., Gupta, S. K., & Pathak, D. D. (2019). Selective adsorption of toxic heavy metal ions using guanine-functionalized mesoporous silica [SBA-16-g] from aqueous solution. Microporous and Mesoporous Materials, 288, 109577. doi:10.1016/j.micromeso.2019.109577.

[38] Zhang, C., Liu, S., Li, S., Tao, Y., Wang, P., Ma, X., & Chen, L. (2019). Enahanced biosorption of Cu(II) by magnetic chitosan microspheres immobilized Aspergillus sydowii (MCMAs) from aqueous solution. Colloids and Surfaces A: Physicochemical and Engineering Aspects, 581, 123813. doi:10.1016/j.colsurfa.2019.123813.

[39] Ren, Y., Abbood, H. A., He, F., Peng, H., & Huang, K. (2013). Magnetic EDTA-modified chitosan/SiO2/Fe3O4 adsorbent: Preparation, characterization, and application in heavy metal adsorption. Chemical Engineering Journal, 226, 300–311. doi:10.1016/j.cej.2013.04.059.

[40] Li, G., Zhao, Z., Liu, J., & Jiang, G. (2011). Effective heavy metal removal from aqueous systems by thiol functionalized magnetic mesoporous silica. Journal of Hazardous Materials, 192(1), 277–283. doi:10.1016/j.jhazmat.2011.05.015.

[41] Repo, E., Malinen, L., Koivula, R., Harjula, R., & Sillanpää, M. (2011). Capture of Co(II) from its aqueous EDTA-chelate by DTPA-modified silica gel and chitosan. Journal of Hazardous Materials, 187(1–3), 122–132. doi:10.1016/j.jhazmat.2010.12.113.

[42] Azizian, S., & Eris, S. (2021). Adsorption isotherms and kinetics. Adsorption: Fundamental Processes and Applications, 445–509, Elsevier, Amsterdam, Netherlands. doi:10.1016/b978-0-12-818805-7.00011-4.

[43] Pearlin Kiruba, U., Senthil Kumar, P., Sangita Gayatri, K., Shahul Hameed, S., Sindhuja, M., & Prabhakaran, C. (2015). Study of adsorption kinetic, mechanism, isotherm, thermodynamic, and design models for Cu(II) ions on sulfuric acid-modified Eucalyptus seeds: temperature effect. Desalination and Water Treatment, 56(11), 2948–2965. doi:10.1080/19443994.2014.966279.

[44] Norfadhilatuladha, A., Tajuddin, M. H., Norhaniza, Y., Jaafar, J., Aziz, F., & Misdan, N. (2017). Penyingkiran Plumbum(II) daripada larutan akues mengunakan gentian nano karbon teraktif poliakrilonitril/zink oksida. Malaysian Journal of Analytical Sciences, 21(3), 619–626. doi:10.17576/mjas-2017-2103-11.

[45] Habiba, U., Siddique, T. A., Li Lee, J. J., Joo, T. C., Ang, B. C., & Afifi, A. M. (2018). Adsorption study of methyl orange by chitosan/polyvinyl alcohol/zeolite electrospun composite nanofibrous membrane. Carbohydrate Polymers, 191, 79–85. doi:10.1016/j.carbpol.2018.02.081.

[46] Phasuphan, W., Praphairaksit, N., & Imyim, A. (2019). Removal of ibuprofen, diclofenac, and naproxen from water using chitosan-modified waste tire crumb rubber. Journal of Molecular Liquids, 294, 111554. doi:10.1016/j.molliq.2019.111554.